Supporting Information

# Water-Assisted Spin-Flop Antiferromagnetic Behaviour of Hydrophobic Cu-Based Metal–Organic Frameworks

Arif I. Inamdar,[a,b,c] Batjargal Sainbileg,[d,e] Saqib Kamal,[a,f] Khasim Saheb Bayikadi,[g] Raman Sankar,[g] Tzuoo Tsair Luo,[a] Michitoshi Hayashi,[d,e]* Ming-Hsi Chiang,[a,c,h]* and Kuang-Lieh Lu[a,i]*

[a] Institute of Chemistry, Academia Sinica, Taipei 115, Taiwan
[b]Department of Applied Chemistry, National Yang Ming Chiao Tung University, Hsinchu 300, Taiwan
[c] Sustainable Chemical Science and Technology, Taiwan International Graduate Program, Academia Sinica, Taipei 115 and National Yang Ming Chiao Tung University, Hsinchu 300, Taiwan
[d] Center for Condensed Matter Sciences, National Taiwan University, Taipei 106, Taiwan
[e] Center of Atomic Initiative for New Materials, National Taiwan University, Taipei 106, Taiwan
[f] Molecular Science and Technology, Taiwan International Graduate Program, Institute of Atomic and Molecular Science, Academia Sinica, Taipei 115 & Department of Chemistry, National Tsing Hua University, Hsinchu 300, Taiwan
[g] Institute of Physics, Academia Sinica, Taipei 115, Taiwan
[h] Department of Medicinal and Applied Chemistry, Kaohsiung Medical University, Kaohsiung 807, Taiwan
[i] Department of Chemistry, Fu Jen Catholic University, New Taipei City 242, Taiwan

**Table of Contents**

Experimental section

Materials and instrumentation

Synthesis

Computational calculations

**Fig. S1** Structure of **1**.

**Fig. S2** PXRD patterns of **1**, **1′** and **1"**.

**Fig. S3** Pore-size distribution of **1′** and **1"**.

**Fig. S4** The $\chi_M$ vs.T and d($\chi_M$T)/dT vs. T plots of **1** in 2–10 K at 100 Oe.

**Fig. S5** ZFC and FC $\chi_M T$ plots at 100 Oe for **1**.

**Fig. S6** Spin density distribution of **1**.

**Fig. S7** Band structures and DOS of **1** and **1"**.

**Fig. S8** Orbital-projected DOS (PDOS) of copper and oxygen atoms in **1** and **1"**.

## Experimental section

### Materials and instrumentations

All chemical and reagents were purchased commercially and were used without further purification. Powder X-ray diffraction data were collected on a Bruker D8 Advance powder diffractometer at 40 kV and 40 mA operating at the Cu Kα wavelength (1.5406 Å). Magnetic susceptibility measurements of powdered samples were performed on a Quantum Design SQUID-VSM magnetometer (Quantum Design, San Diego, CA, USA) in the temperature range of 2–300 K at 5000 Oe. For the field dependent magnetic susceptibility measurements, the data were collected at 2 K under various applied fields. The data were corrected for the diamagnetic contribution of the sample holder using experimentally obtained gram susceptibility data. Molar susceptibility data were corrected for diamagnetic contributions using the Pascal constants.[1] Nitrogen adsorption-desorption isotherms of MOF **1′** and **1"** were measured on a Micromeritics ASAP 2020 at 77 K by the volumetric method. The samples were degassed at 353 K for 6 hr under vacuum before measurements. The Brunauer-Emmett-Teller (BET) and Barrett-Joyner-Halenda (BJH) analyses were used to estimate surface area and pore volumes. FT-IR measurements were carried out on a Perkin-Elmer Model Paragon 1000 FT-IR spectrometer in the range of 400–4000 $cm^{-1}$. Elemental analyses were performed on a Perkin-Elmer 2400 CHN analyzer.

### Synthesis

MOF **1**, **1′** and **1"** were synthesized based on previously reported methods.[2] Basic $CuCO_3(OH)_2$ (22 mg, 0.1 mmole) and 4,4'-(hexafluoroisopropylidene) diphthalic anhydride (HFDPA) (22 mg, 0.05 mmole) and 8 mL water were placed in a glass tube which was then sonicated for 5 minutes. The mixture was then allowed to stand in an 80 °C water bath for three days. A crystalline sample was formed and collected, which is referred as MOF **1**. MOF **1′** and **1"** were prepared by heating **1** under a vacuum at two different temperatures, 140 °C and 170 °C. The sample with guest water molecules removed at 140 °C is referred as **1′**. At 170 °C, both of the guest and coordinated water molecules were removed. The sample prepared at this temperature is referred as **1"**.

## Computational details of DFT calculations

The first-principles DFT calculations for MOF **1** and **1"** were carried out via the Vienna *ab-initio* simulation package (VASP 5.4.4), within a plane-wave basis set and projector augmented wave (PAW) potential methods.[3] The accurate hybrid exchange-correlation functional including Perdew–Burke–Ernzerhof method with the Coulomb U parameter (PBE+U) and Grimme's D3 dispersive correction (PBE-D3) was employed for all spin-polarized simulations. The on-site Coulomb U parameter was applied at 7 eV as in previous common studies, in order

to precisely account for the *d* electrons of copper ions. The threshold for a self-consistent energy convergence of $10^{-5}$ eV and a force convergence of $10^{-3}$ eV/Å was used for structure optimizations. The first Brillouin zone is sampled with the Monkhorst-Pack 10 × 4 × 6 k-point meshes together with the energy cutoff of 500 eV for all DFT calculations.

The short Cu•••Cu contacts and Cu–O distances for which the Cu1•••Cu2, Cu1•••Cu3, and Cu3•••Cu4 distances are 3.068, 3.021, and 3.158 Å, respectively, and M–O bond distance is ~2 Å, are capable of mediating electronic communication (Fig. S1a–c).

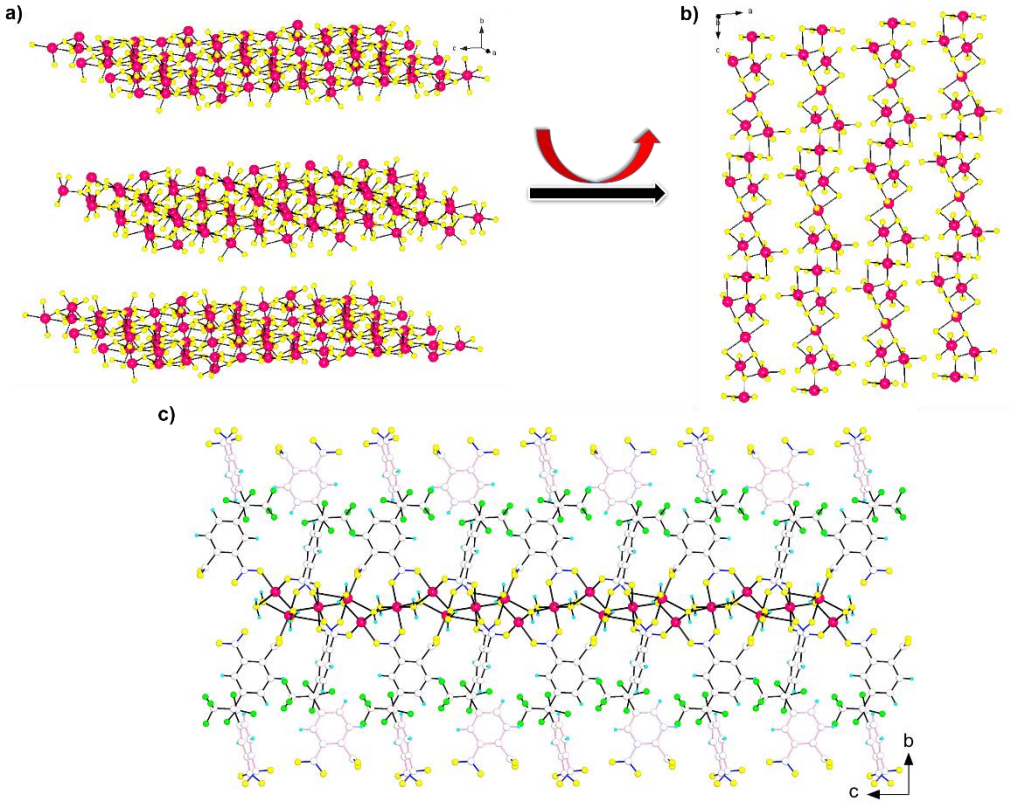


**Fig. S1** a) Structure of **1**, forming metal sheets. b) Inverted representation of **1**. c) Metal oxide chains showing the arrangement of the Cu (II) centres.

## Effects of the dehydration process on the structures and magnetic property of MOFs

The structure of crystalline compound **1** at the {020} plane shrinks to some extent upon the removal of the guest water molecules. A new peak attributed to compound **1′** emerges at 2θ = 6.45°. The peak at 2θ = 6.03° originated from compound **1** disappears after on the removal of guest and coordinated water molecules. A slight misalignment of the metal-carboxylate chains of the framework for the adjustment of the volume shrinkage that occurs due to the dehydration process. This results in the peak shift for the 2θ = 6.03° signal and the appearance of new signals at 2θ = ~15°, ~17.5°, ~23.8° and ~36.3°. The previous PXRD results for MOFs show a similar behaviour.[4,5]

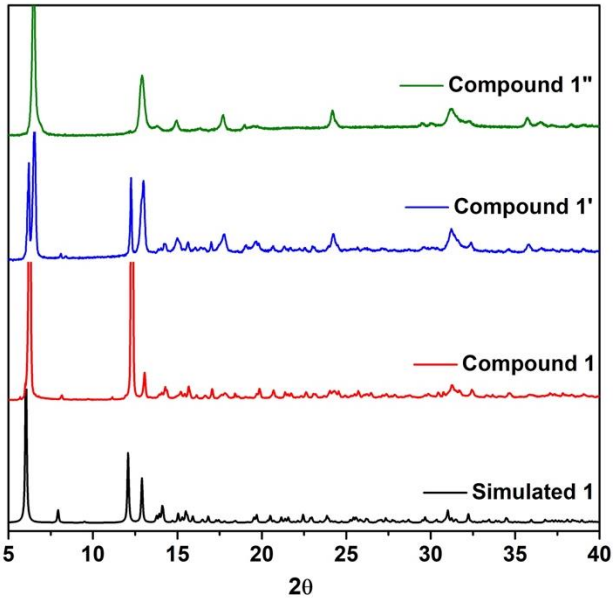


**Fig. S2** PXRD patterns of MOF **1**, **1′**, **1"** and the simulated pattern of **1**.

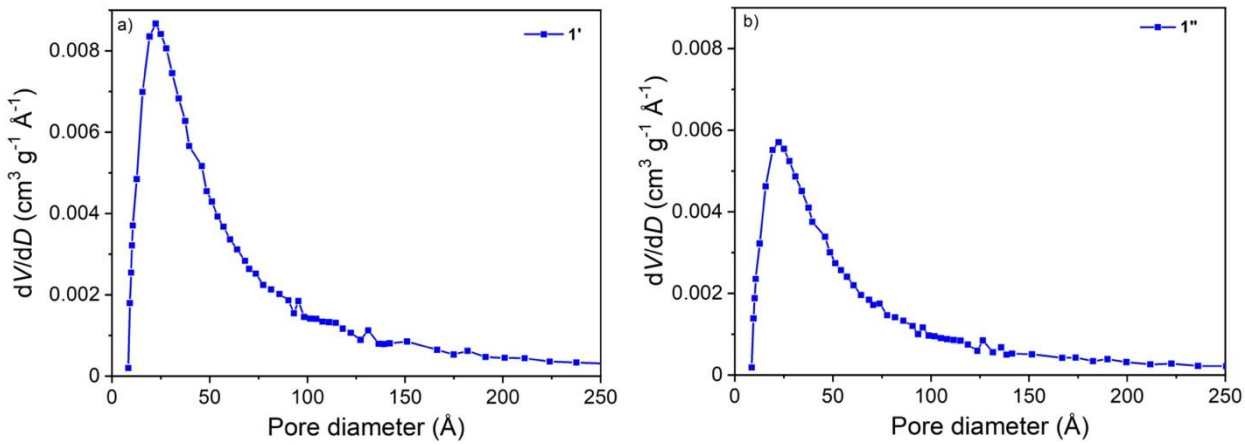


**Fig. S3** Pore-size distribution of a) **1′** and b) **1"**. The BJH pore volume of **1′** and **1"** is 0.5533 and 0.3698 $cm^3\ g^{-1}$, respectively.

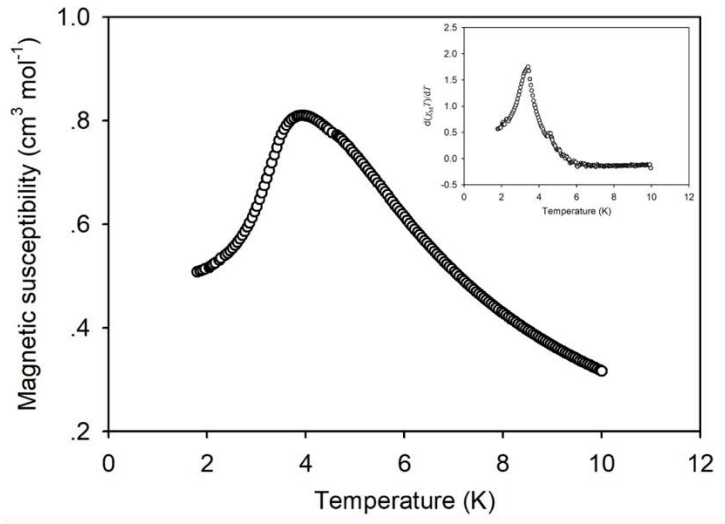


**Fig. S4** The plot of magnetic susceptibility vs. temperature for **1** in 2-10 K at 100 Oe. Inset: a plot of d($\chi_M$T)/dT vs. temperature is shown.

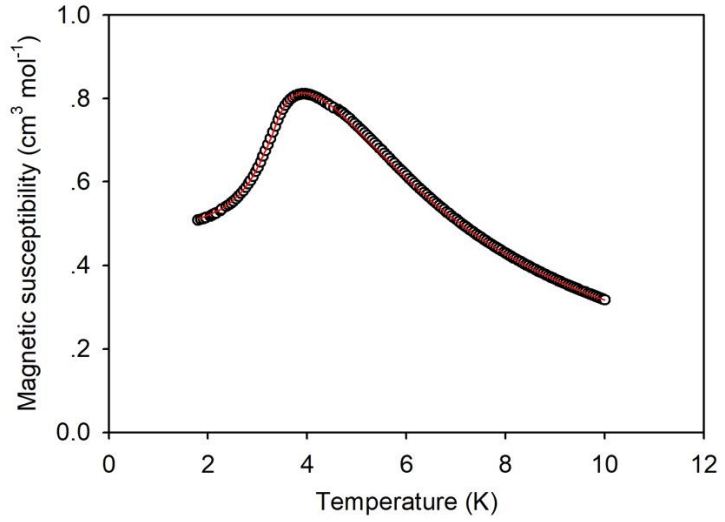


**Fig. S5** Temperature-dependent zero-field cooling (ZFC, black circles) and field-cooling (FC, red line) $\chi_M T$ plots at 100 Oe for **1**.

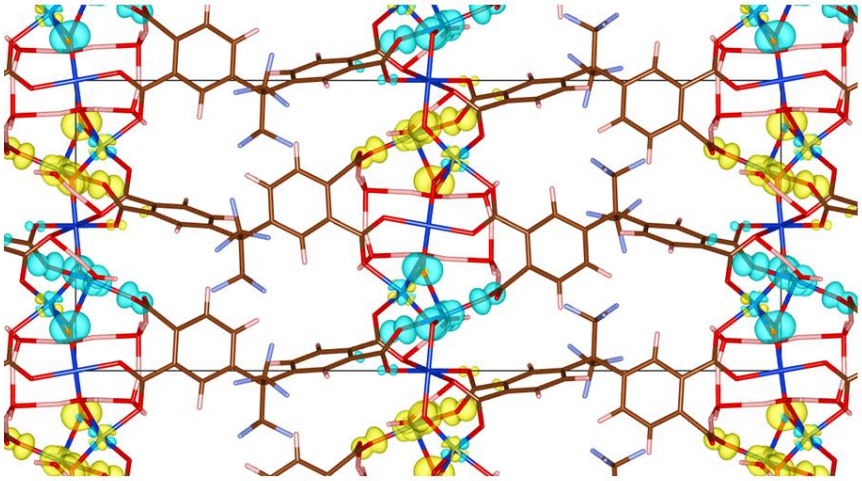

**Fig. S6** Spin density distribution of **1** where yellow and cyan isosurfaces represent the positive and negative regions of spin density, respectively. Spin densities are mainly accumulated on Cu-ion whereas some spin-polarized distributions are observed on the O atoms which are directly bonded to Cu-ions. The black box represents the boundary of the periodic cell of the crystal structure.

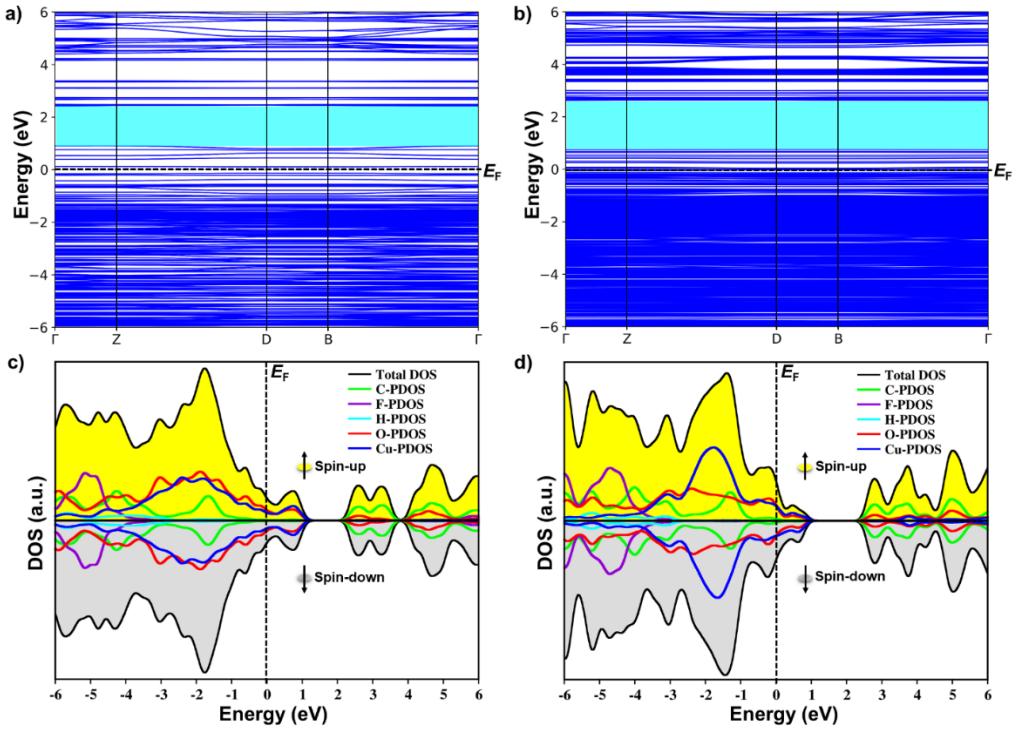


**Fig. S7** a-b) Band structures and c-d) DOS of **1** and **1**. The dashed line at 0 eV illustrates the Fermi level $E_F$. The bandgap of **1** and **1**" is 1.6 eV and 1.9 eV, respectively.

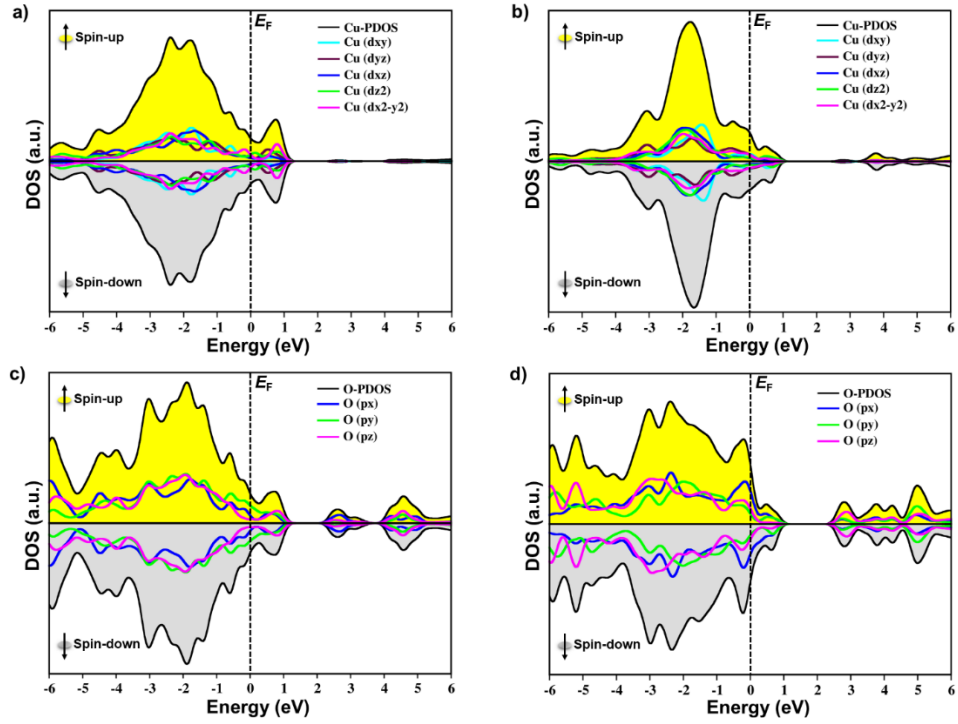


**Fig. S8** Orbital-projected DOS (PDOS) of a) copper and c) oxygen atoms in **1**. PDOS of b) Cu and d) O atoms in **1**".

**References**


1. G. A. Bain and J. F. Berry, *J. Chem. Educ.*, 2008, **85**, 532-536.
2. A. I. Inamdar, A. Pathak, M. Usman, K. R. Chiou, P. H. Tsai, S. Mendiratta, S. Kamal, Y. H. Liu, J. W. Chen, M.-H. Chiang and K. L. Lu, *J. Mater. Chem. A*, 2020, **8**, 11958–11965.
3. G. Kresse and J. Hafner, *Phys. Rev. B*, 1993, **47**, 558–561.
4. N. Klein, C. Herzog, M. Sabo, I. Senkovska, J. Getzschmann, S. Paasch, M. R. Lohe, E. Brunner and Stefan Kaskel, *Phys. Chem. Chem. Phys.*, 2010, **12**, 11778–11784.
5. P. Schmieder, D. Denysenko, M. Grzywa, O. Magdysyuk and D. Volkmer, *Dalton Trans.*, 2016, **45**, 13853–13862.